A QUASI-COULOMB MODEL FOR FRICTIONAL CONTACT INTERFACES

C. García Garino
Instituto Tecnológico Universitario, UNC
Parque General San Martín, 5500, Mendoza, Argentina
e–mail: cgarcia@pascal.uncu.edu.ar

J.-P. Ponthot and R. Boman
L.T.A.S. – Milieux Continus & Thermomcanique
Universit de Lige, B-4000 Lige, Belgium
e–mail: jp.ponthot@ulg.ac.be r.boman@ulg.ac.be

J. Oliver
E T. S. de Ingenieros de Caminos Canales y Puertos
Gran Capitán s/n, E-08034, Barcelona, Spain

ABSTRACT

Frictional contact interfaces have to be modeled in practice when industrial problems such as metal forming operations, crashworthiness, and so on, have to be simulated. Usually a Coulomb model is used in order to describe the constitutive law for the frictional case. Following a standard plasticity approach to Coulomb law a non-symmetric tangent operator is found, and so a non-symmetric solver has to be used in order to take full advantage of consistent operators. With respect to symmetric ones, these non-symmetric operators lead to prohibitive computational times. However, in practice different schemes have been proposed in order to recover the symmetric operator, and consequently, use a symmetric solver. In this work an alternative approach based on an idea due to García Garino and Oliver[33] is defined in order to avoid to deal with non-symmetric solvers and thus save a large amount of computational time, which renders the computational simulation more attractive to industry. Applications to metal forming simulations and crashworthiness analysis are envisaged.

INTRODUCTION

The Finite Element Method[3,33] can be considered as a valuable tool in order to simulate large industrial applications. In the last few years very important progress has been reported in the simulation of non linear problems involving plasticity and large strains, as can be seen in the proceedings of Computational platicity conferences.[18–22]

In many cases the simulation of manufacturing processes like metal forming[9,22,26] requires to take into account besides non linear constitutive models complex boundary conditions like frictional contact interfaces.[2,8,31] Another important field of research when this kind of interfaces are required is Crashworthiness.

The contact problem involves the interface of two deformable bodies or a deformable body against a rigid tool (unilateral contact). In both cases one the body is prevented from penetrating the other, consequently the possible configuration and displacement fields are constrained in the admissible values to be reached.

From the mathematical point of view the mechanical problem stated in the previous paragraph can be considered like an optimization problem and several methods can be found in the literature: Penalty method,[13–15,24] Lagrange Multipliers[4,5] and Perturbed Lagrange Formulations[28] from which the two others method can be derived and Augmented Lagrangian formulation.[27,30]

The frictional behaviour is ususally taken into account in Computational Mechanics by mean of elastoplasticity analogy,[10] and in the last years Wriggers and coauthors[29,31] have derived very efficient numerical tools extended the Radial Return algorithm to this context. A review of the subject can be found, among others, in Agelet[1] and Zhong.[32]

The frictional contact problem can be stated enhancing the variational unconstrained problem in order to include the contact and friction contributions. The Finite Element Method lets to write the corresponding discretized problem adding to the Stiffness Matrix $\boldsymbol{K}$ and residual forces $\boldsymbol{R}$ the contact contributions $\boldsymbol{K_c}$ and $\boldsymbol{R_c}$ respectively and friction is taken into account by mean of $\boldsymbol{F_f}$ and $\boldsymbol{R_f}$ respectively. The standard treatment of frictional problem is ususally modelled using a Coulomb model that leads to a non-symmetric Stiffnes matrix, consequently non-symmetric solvers have to be used in the numerical simulation.

However, recovering a symmetric operator is possible. In that sake, Garcia-Garino and Oliver[11,12] proposed an algorithm, called Quasi-Coulomb model, able to integrate the frictional equations in time and that leads to a symmetric tangent operator. Laursen and Simo[16,27] have proposed anothers ideas in order to get a symmetric operator for the contact frictional problem based on Coulomb law.

The capabilities of this new algorithm are analysed in this paper by solving several large deformation problems pertaining to metal forming simulation and crashworthiness analysis. A penalty formulation and two differente large strain elastoplastic numerical models developed by the authors are used.[11,23]

Anyway, in order to simulate realistic industrial forming simulations, a bulk model is not sufficient and a frictional algorithm has to be implemented. The role of this algorithm is to manage the contact and frictional forces that appear due to material-tools interactions. Details of such an algorithm, which is equivalent for both hyper and hypo-elastic approaches can be found in[8,9,21]

The contact algorithms are generally based on a standard plasticity approach[2] but with a non-associated flow rule. If one uses an implicit algorithm in order to integrate the motion equations in time, the resulting tangent operator is non-symmetric, due to the non-associated flow rule. This leads to prohibitive computational times.

FRICTIONAL CONTACT INTERFACE

Governing equations

In many practical problems the boundary conditions have to include the case of frictional contact problems such as the interface solid-tools. In this case the unconstrained finite strain quasi-static elastoplastic problem written in terms of the internal forces resulting from the straining of the material (i.e. the so-called stress-divergence term), denoted by $\boldsymbol{G}(\boldsymbol{u})$ as a function of the nodal displacements $\boldsymbol{u}$ and the external load pattern $\boldsymbol{F}$ results in (see e.g. Zienkiewicz, Bathe[3,33] for details):

$$\boldsymbol{G}(\boldsymbol{u}) - \boldsymbol{F} = 0 \tag{1}$$

Equation (1) is then enhanced by means of contact and frictional nodal forces respectively denoted by $\boldsymbol{R_C}$, and $\boldsymbol{R_F}$ to account for contact interactions (see Zhong[32] and the references therein for details). The constrained problem results:

$$\boldsymbol{G}(\boldsymbol{u}) + \boldsymbol{R_C}(\boldsymbol{u}) + \boldsymbol{R_F}(\boldsymbol{u}) - \boldsymbol{F} = 0 \tag{2}$$

In case of a dynamic problem, inertia forces have to be taken into account. In such a case, the semi-discretized equation to be integrated reads, see Bathe,[3] Belytschko[7] for details:

$$\boldsymbol{M}\ddot{\mathbf{u}} + \boldsymbol{G}(\boldsymbol{u}) + \boldsymbol{R_C}(\boldsymbol{u}) + \boldsymbol{R_F}(\boldsymbol{u}) - \boldsymbol{F} = 0 \tag{3}$$

where $\boldsymbol{M}$ is the mass matrix and $\ddot{\boldsymbol{u}}$ is the vector of nodal accelerations.

Because of combined geometrical, material and contact non linearities, the systems of equations (2) and (3) are highly non linear in $\boldsymbol{u}$. The methods of solution of these systems are standard (Bathe,[3] Belytschko[7]) and, in numerous cases Newton-Raphson's method has proved to be advantageous.

Frictionless contact problem

Attention is now focused on the plannar and axisymmetric case of a straight rigid tool boundary $\boldsymbol{x_2}^T - \boldsymbol{x_1}^T$ (where T stands for tool), for simplicity. The extension to three dimensional problems is straightforward and all the following formula are valid in 2D, as well as 3D situations.

The constraint equations resulting from contact interactions are based on nodal imposition of the constraint for every slave node pertaining to the boundary of the finite element mesh. In this context, and with reference to figure 1, the gap or penetration is approximated by the finite element method nodally. Here, the gap g, associated with a typical slave node $\boldsymbol{x_s}$ is given by:

$$g = (\boldsymbol{x_s} - \boldsymbol{x_1}^T) \cdot \boldsymbol{N} \tag{4}$$

where $\boldsymbol{N}$ denotes the unit outward normal to the tool segment. Similarly $\boldsymbol{T}$ denotes the unit tangent to this segment, see figure 1. In 3D situations, $\boldsymbol{T}$ defines the local tangent plane to the contact point.

If g is larger than zero, there is no contact between the considered slave node and the segment and, consequently $\boldsymbol{R_C} = 0$ and $\boldsymbol{R_F} = 0$. However, if $g \leq 0$, there exists a contact interaction that has to be accounted for, as described hereafter.

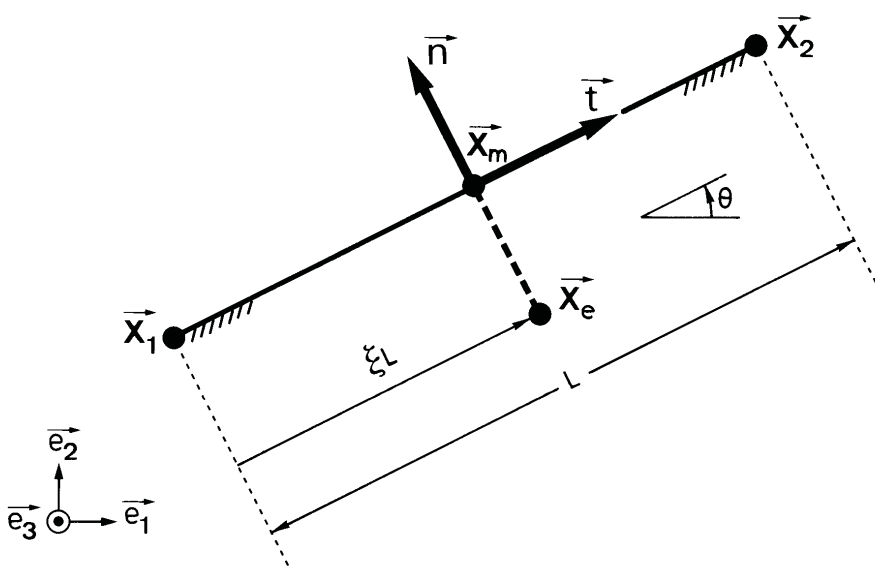

Figure 1: Geometry of the contact problem

The nodal forces $\boldsymbol{R_C}$ arising from contact are computed using the penalty method.[13–15,24] In local axis the normal contact force t_N results in:

$$t_n = \epsilon_c g \quad if \;\; g \leq 0 \tag{5}$$

$$t_n = 0 \;\; if \;\; g < 0 \tag{6}$$

where ϵ_c stands for normal penalty coefficient. This resulting force is written in global coordinates as:

$$\boldsymbol{R_C} = t_N \boldsymbol{N} \tag{7}$$

In the case of rigid flat tools there are no changes in the geometry of the tool from one iteration to another and the contact contribution to the stiffness matrix of the problem, i.e. the derivative of $\boldsymbol{R_C}$ with respect to $\boldsymbol{\Delta u}$, the incremental nodal displacement, reads:

$$\boldsymbol{K_C} \;=\; \frac{\partial \boldsymbol{R_C}}{\partial \Delta \boldsymbol{u}} \;=\; \epsilon_c\, \boldsymbol{N}\boldsymbol{N}^T \qquad if \quad g \leq 0 \tag{8}$$

Frictional contact problem

In this problem two cases can be distinguished: in early stages of the process, where a full stick condition between the solid and the tool is verified, a tangential force that opposes to the relative slip appears. Once a treshold value in the modulus of the force is reached, a slip condition is verified. This behaviour can be modelled by means of the classical Coulomb law:

$$\boldsymbol{t_F} = -sign(\dot{\boldsymbol{u}})\|\boldsymbol{t_F}\|\boldsymbol{T} \tag{9}$$

and

$$\|\boldsymbol{t_F}\| \;\leq\; \mu \;|t_N\;| \tag{10}$$

where $\|\boldsymbol{t_F}\| < \mu|t_N|$ in case of sticking contact and $\|\boldsymbol{t_F}\| \;=\; \mu|t_N|$ in case of sliding contact. In order to perform a numerical integration of the frictional behaviour, we proceed as follows. Starting from a known configuration at time t, one is faced with determining a new equilibrated configuration at time $t + \Delta t$. As far as the frictional treatment is concerned, Coulomb's law can be regularized by introducing a penalty factor ϵ_F. In this way, the problem can be treated similarly to an elastoplastic one, see Curnier.[10] The tangential slip $\boldsymbol{s}$ is thus decomposed into its elastic (reversible) and plastic (irreversible) components

$$\boldsymbol{s} = \boldsymbol{s^e} + \boldsymbol{s^p} \tag{11}$$

so that, by analogy with elasto-plasticity, the constitutive equation for the frictional component can be written, in the tangential plane of contact

$$\boldsymbol{t_F} \;=\; \epsilon_F \;=\; \epsilon_F.(\boldsymbol{s} - \boldsymbol{s^p}).\boldsymbol{s^e} \tag{12}$$

Further, following Wriggers et al.,[29,31] an elastic predictor is evaluated by supposing that the entire incremental slip, resulting from the finite element computation, is totally reversible (elastic). This results in an elastic (sticking) predictor ${}^{t+\Delta t}\,\boldsymbol{t_F}^{TR}$ for the frictional force given by

$${}^{t+\Delta t}\boldsymbol{t_F}^{TR} = {}^{t}\boldsymbol{t_F} + \epsilon_F \Delta \boldsymbol{s}^{\boldsymbol{e}TR} \tag{13}$$

This elastic predictor is then compared with the Coulomb criterion (10). If $\|{}^{t+\Delta t}\boldsymbol{t_F}^{TR}\| \leq \mu|{}^{t+\Delta t}t_N|$, the state of contact was clearly an elastic one and nothing more is undertaken. On the contrary, if $\|{}^{t+\Delta t}\boldsymbol{t_F}^{TR}\| > \mu^{t+\Delta t}|t_N|$, i.e. Coulomb criterion is violated, the state of contact is sliding and a correction has to be evaluated to restore consistency with the Coulomb criterion. This is done by integrating the following flow rule for the frictional components:

$$\boldsymbol{s^p} = \lambda \boldsymbol{T} \tag{14}$$

So that the final frictional force will be given by:

$${}^{t+\Delta t}\boldsymbol{t_F} = \epsilon_F\;(\boldsymbol{s^e} - \lambda\;\boldsymbol{T}) = {}^{t+\Delta t}\boldsymbol{t_F}^{TR} - \epsilon_F\;\lambda\;\boldsymbol{T} \tag{15}$$

Assuming $\boldsymbol{T} \;=\; \dfrac{\boldsymbol{t_F}^{TR}}{\|\boldsymbol{t_F}^{TR}\|}$, an hypothesis consistent with the radial return scheme of elastoplasticity, the norm of (15) can be shown to be:

$$\|{}^{t+\Delta t}\boldsymbol{t_F}\| = \|\boldsymbol{t_F}^{TR}\| - \epsilon_F \; \lambda \tag{16}$$

The unknown λ is computed by inserting (16) into the Coulomb criterion (10), i.e.

$$\|{}^{t+\Delta t}\boldsymbol{t_F}^{TR}\| - \epsilon_F \; \lambda - \mu \; |{}^{t+\Delta t}t_N| \; = 0 \tag{17}$$

If the friction coefficient μ is constant the latest equation has a closed form solution and the classical expression of the Coulomb law is recovered:

$$\|{}^{t+\Delta t}\boldsymbol{t_F}\| = \mu \; |{}^{t+\Delta t} \; t_N| \tag{18}$$

Writing the nodal forces $\boldsymbol{R_F} = signt_F \|\boldsymbol{t_F}\| \; \boldsymbol{T}$, where $signt_F$ is a function that accounts for the sign of tangencial forces. The frictional contribution to nodal forces and stiffness matrix results:[29]

$$\boldsymbol{K_F} = \begin{cases} \epsilon_F \;\; \boldsymbol{T} \;\; \boldsymbol{T^T} & \text{if} \quad \|\boldsymbol{t_F}\| < \mu \; |t_N| \\ -\mu \; \epsilon_C \;\; \boldsymbol{T} \;\; \boldsymbol{N^T} & \text{if} \quad \|\boldsymbol{t_F}\| = \mu \; |t_N| \end{cases} \tag{1}$$

In the second case, i.e. in the case of sliding contact, $\boldsymbol{K_F}$ is obviously non-symmetric.

To avoid the use of non symmetrical solvers, which are computationnally much more expensive than symmetrical ones, the standard procedure is modified and the modulus of the normal reaction is no longer updated at each equilibrium iteration. This modulus remains constant all over the load step and equals to the latest converged value. Then the equation (20) describes a Quasi-Coulomb friction law[11,12] of the type:

$$\|{}^{t+\Delta t}\boldsymbol{t_F}\| \;\; = \;\; \mu \;\; |{}^{t} \; t_N| \tag{20}$$

and the discretized Coulomb law (17) can be approximated by:

$$\|{}^{t+\Delta t}t_F^{TR}\| - \epsilon_F \; \lambda - \mu \; |{}^{t}t_N| \; = 0 \tag{21}$$

In practice this simplificative assumption is equivalent to approximate in a stepwise way the yield function given by the equation (10), as can be seen in 2:

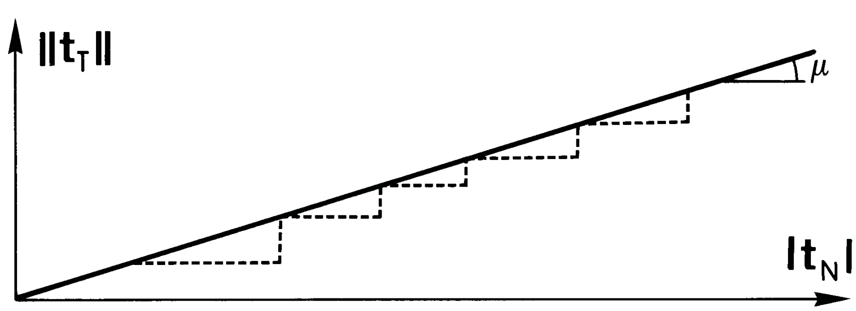

Figure 2: Original (solid line) and modified (dotted line) yield criteria

It is important to mention that the flow rule is not changed and the problem becomes associated, consequently a symmetric stiffness matrix is obtained. Morover if the three following conditions are fullfilled:

- i) Elastic-perfectly plastic problem (μ constant)
- ii) Linear geometry (rigid tools)
- iii)A Quasi-Coulomb law is used.

the frictional matrix $\boldsymbol{K_F}$ since in this case:

$$\boldsymbol{K_F} = \frac{\partial \boldsymbol{R_F}}{\partial \Delta \boldsymbol{u}} = \frac{\partial \mu}{\partial \Delta \boldsymbol{u}} \, {}^t t_N \, \boldsymbol{T} \, + \, \mu \, \frac{\partial \, {}^t t_N}{\partial \Delta \boldsymbol{u}} \, \boldsymbol{T} + \, \mu \, {}^t t_N \, \frac{\partial \boldsymbol{T}}{\partial \Delta \boldsymbol{u}} \, = 0 \tag{22}$$

because all the variables are fixed.

NUMERICAL SIMULATION

In order to investigate the effects of the symmetrisation process on the accuracy of the results, three benchmarks have been tested. They are presented below. Of course, in case of frictionless problems, this symmetrisation process has no influence since the Hessian is already symmetric.

Stretching of an axisymmetric sheet with an hemispherical punch

The first example studied is a benchmark problem proposed by Lee, Wagoner and Nakamichi[17] from OSU (Ohio State University). The problem is a sheet forming simulation and consists of the stretching of an axisymmetrical sheet with an hemispherical punch whose geometry is given in fig. 3. The material is supposed to behave like a J2 elastic-plastic material with non linear isotropic hardening. The material parameters are given in table 1. This kind of material exhibits a very large hardening rate in the neighbourhood of the initial yield stress.

Young Modulus	E =	69004 Mpa
Poisson ratio	ν =	0.3
Yield Stress	σ_v =	$589 \; (0.0001 \; + \; \bar{\epsilon}_p)^{0.216}$ Mpa

The finite element mesh used is a rather coarse finite element mesh as imposed by the benchmark designers. It is shown in fig. 4 and consists of 2 layers of 14 elements each. The elements are bilinear and use a constant pressure to avoid locking. Boundary conditions are also shown in fig. 4. Contact conditions are imposed through a penalty formulation with the following parameters: $\epsilon_C = 10^5 N/mm$ and $\epsilon_F = 10^4 N/mm$. Three friction coefficients have been considered in the present study, i.e $\mu = 0.0$; $\mu = 0.15$ and $\mu = 0.30$. Many results and comparisons with other authors regarding this problem can be found in.[11,23] However, we will concentrate here on the Quasi Coulomb algorithm.

The comparison of the total force applied by the punch as a function of punch displacement is given in fig. 5 for $\mu = 0.30$ (upper curves) and $\mu = 0.15$ (lower curves) for both classical non-symmetric operator and the symmetric Quasi-Coulomb algorithm presented here. This figure shows an excellent agreement between both algorithms. This agreement in turn proofs the higher efficiency of the Quasi-Coulomb algorithm since it only requires a symmetric solver which is much cheaper to use than a non-symmetric one.

However, using a symmetric operator where the actual tangent operator is non symmetric can affect the rate of convergence of the Newton-Raphson algorithm. As shown in table 2, using a symmetric operator only affects moderately this rate of convergence.

	$\mu = 0.0$		$\mu = 0.15$		$\mu = 0.30$	
Operator	Steps	Iter	Steps	Iter	Steps	Iter
Symmetric	101	301	65	173	67	194
Non-symmetric	101	301	58	158	66	189

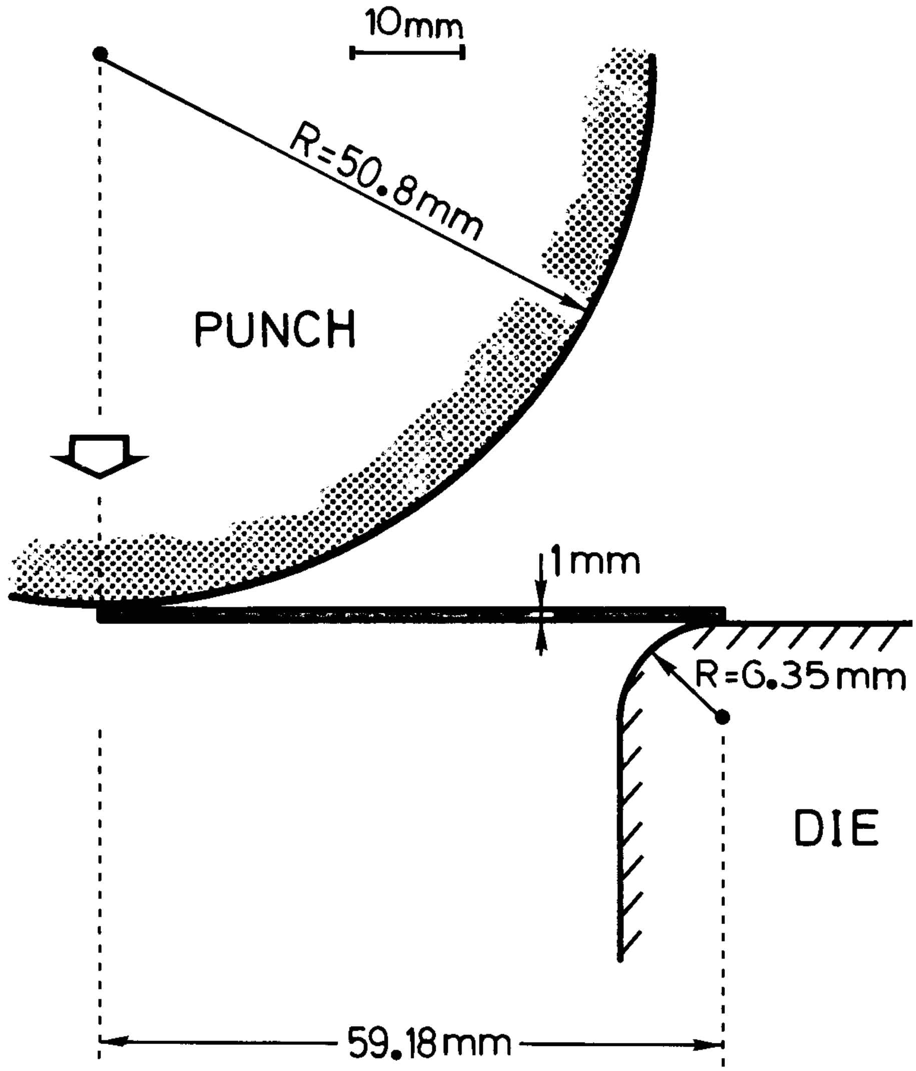

Figure 3: Sheet forming problem: geometry

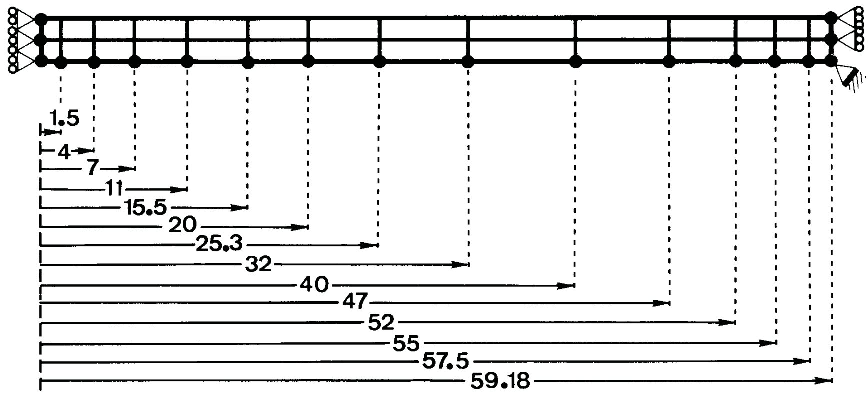

Figure 4: OSU Sheet forming problem: Initial mesh

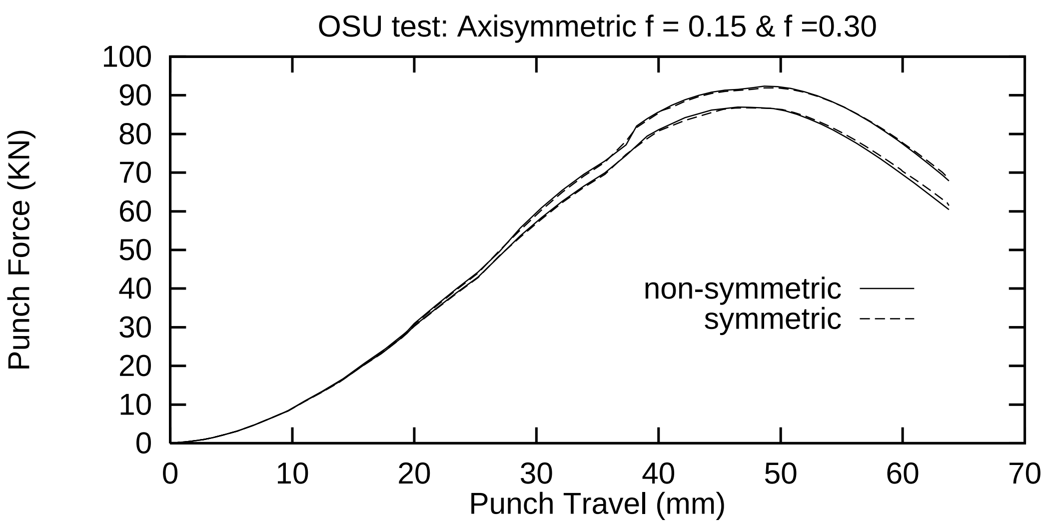

Figure 5: Axisymmetric OSU benchmark: Applied punch force as a function of punch displacement. Top: $\mu = 0.30$, bottom $\mu = 0.15$.

The agreement for Coulomb and Quasi-Coulomb models is not only excellent for the forces (see figure 5), but also as far as local values, like the effective plastic strain are concerned (see figures 6 and 7). On these figures, the results obtained by the classical Coulomb and the Quasi-Coulomb models are compared. Results obtained by Agelet de Saracibar[1] are also plotted.

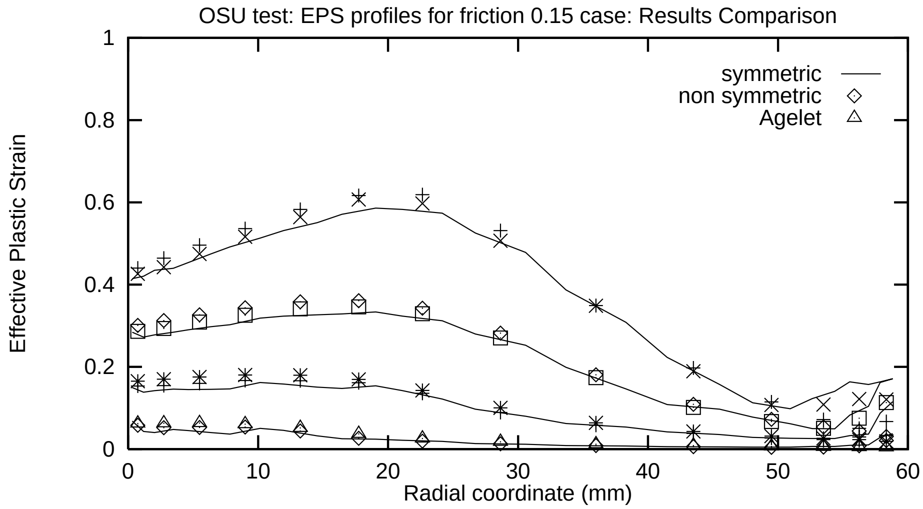

Figure 6: Axisymmetric OSU benchmark. Comparison of plastic strain profile, as a function of initial radius, for punch displacements of 10, 20, 30 and 40 mm. $\mu = 0.15$.

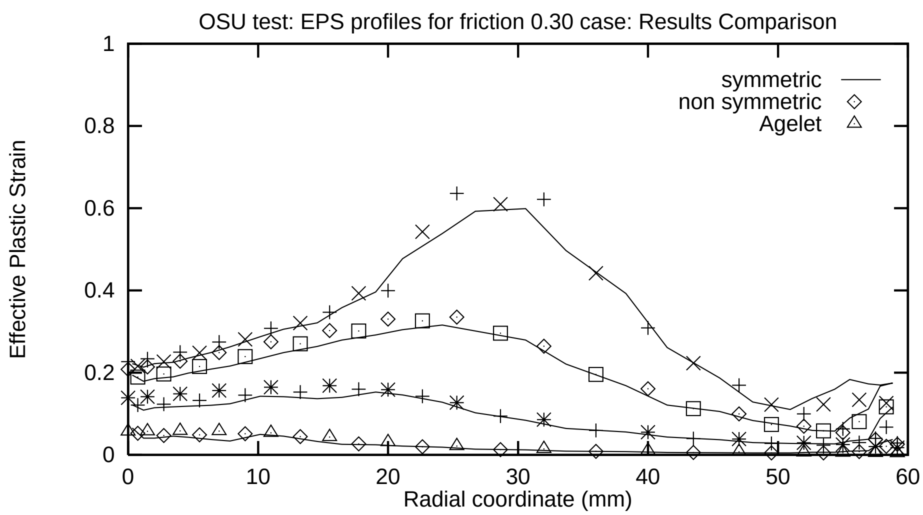

Figure 7: Axisymmetric OSU benchmark. Comparison of plastic strain profile, as a function of initial radius, for punch displacements of 10, 20, 30 and 40 mm. $\mu = 0.30$.

Shock absorber device

This second example deals with the numerical modelling of a shock absorber device. It is based on the turning inside-out of a thin walled ductile metal tube. This is generally called an "invertube" device. In this case (fig. 8.), a plain tube is confronted with a hard die to produce the inversion. This inversion, in turn, produces very large plastic strains which form an efficient energy absorbing mechanism during impact. In this way, the kinetic energy of the impacting bodies is dissipated through plastic deformation, in a controlled fashion at an acceptable rate. The yield limit of the material keeps the transmitted force below an acceptable upperbound. Hence, the deceleration is slower and less harmful for the people inside the car.

Numerical modelling of the collapse of such energy dissipating structures requires not only to take into account the plastic behaviour of the tube material, as well as inertial forces, but also to consider very large strains and large amplitude rigid body motions that develop and also, in this case, the accurate prediction of frictional forces. Thus a great number of advanced code capabilities are tested by running this kind of problems.

Similar problems were investigated by Beltran and Goicolea,[6] by Garcia-Garino[11] with an explicit scheme and by Ponthot & Hogge[25] who compared the performances of explicit and implicit algorithms for impact problems. However, all the previous references dealt with frictionless contact. In the present paper, implicit schemes, as described in[25] have been used to integrate the equations of motion in time. The initial geometry of the system is given in fig. 8.

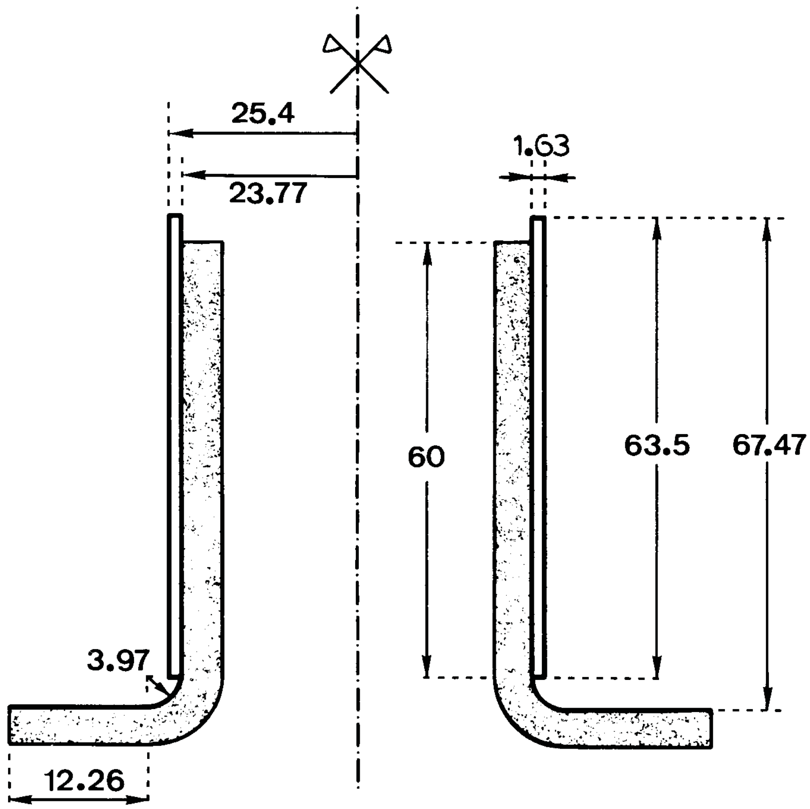

Figure 8: Axisymmetric shock absorber device. All dimensions are in mm. The shaded area is considered to be rigid

The material consists of an aluminium tube of 50.8 mm outside diameter times 63.5 mm length times 1.63 mm wall thickness. The material is supposed to behave like a J2 elastic-plastic material with linear isotropic hardening. The material parameters are given in table 3.

Young Modulus	$E\ =$	67000 Mpa
Poisson ratio	$\nu\ =$	0.33
Density	$\rho\ =$	$2700\frac{kg}{m^3}$
Yield Stress	$\sigma_v\ =$	$15\ +\ 44.7\ \bar{\epsilon}_p$ Mpa

The tube has been modelled using 300 quadrilateral elements (3 x 100) with 4 Gauss points and constant pressure to avoid locking. It is driven against a 3.97 mm radius die made of mild steel at a velocity of 44 m/s (144 Km/h). Thus a 50 mm prescribed vertical displacement over a time period of 0.00125 seconds is imposed on the upper nodes of the tube.

The history of the deformation is given in figures 9, 10 and 11 for $\mu = 0$, $\mu = 0.15$ and $\mu = 0.30$ cases respectively, and a comparison of the final configurations for the three different friction coefficients is given in fig. 12. For this simulation, the following penalty parameters have been used: $\epsilon_C = 10^7 N/mm$ & $\epsilon_F = 10^6 N/mm$.

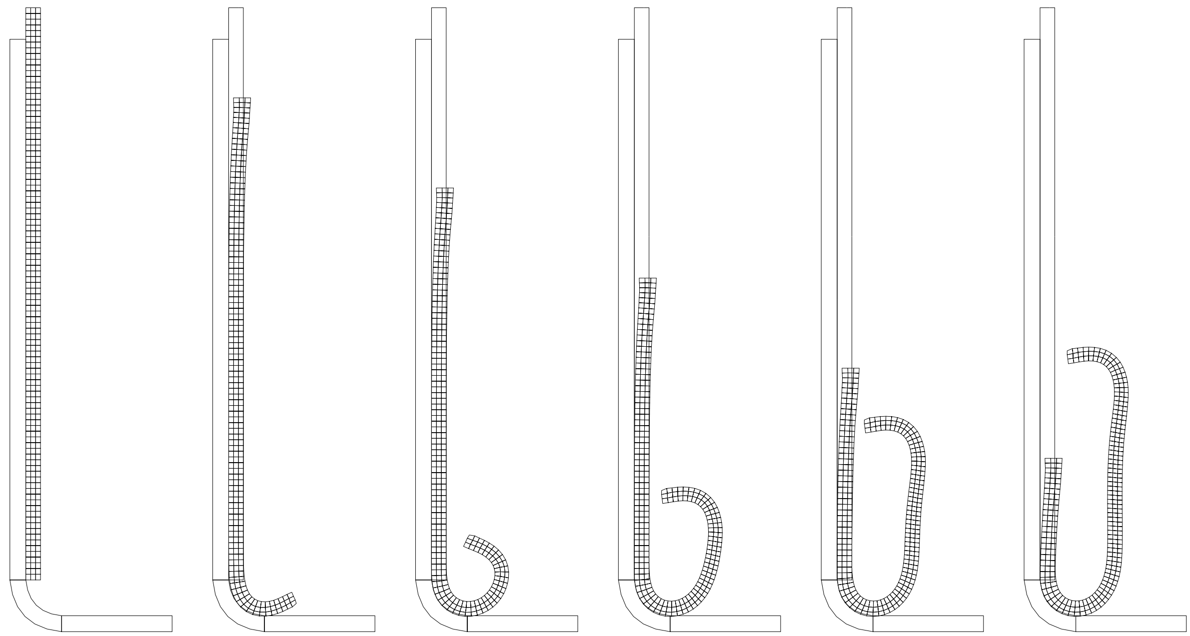

Figure 9: Deformed configurations (frictionless case) for t=0.00, t=0.25, t=0.50, t=0.75, t=1.00 and t=1.25 milliseconds.

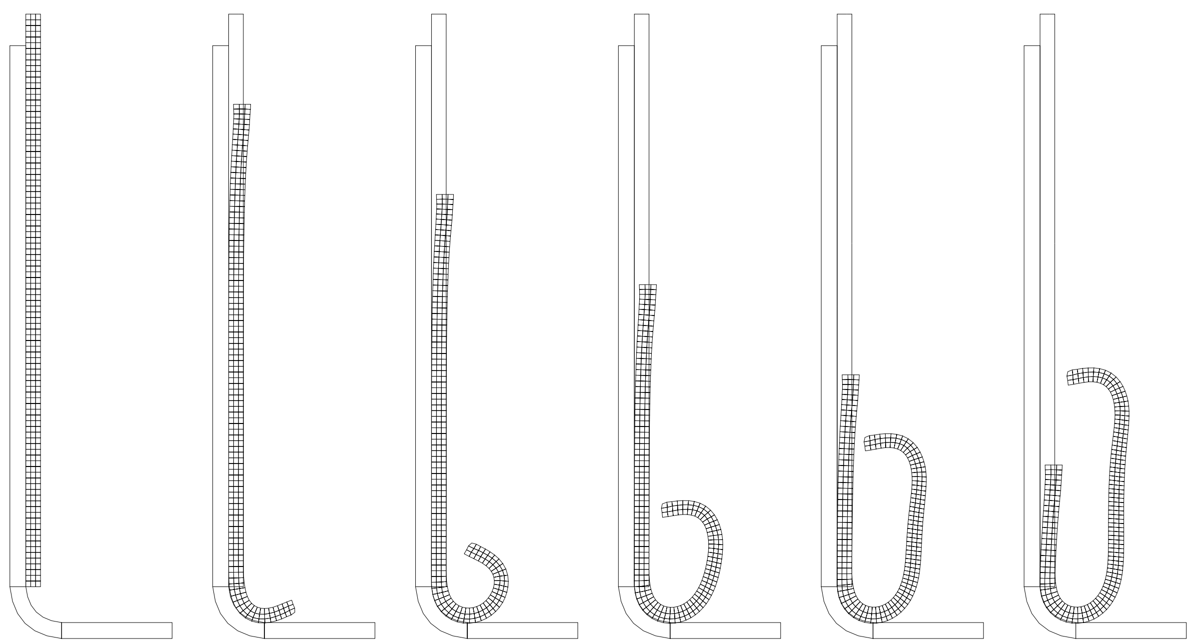

Figure 10: Deformed configurations $\mu = 0.15$ for t=0.00, t=0.25, t=0.50, t=0.75, t=1.00 and t=1.25 milliseconds.

In figure 13 are displayed the time/load curves obtained for the three coefficients of friction and, in each case, for the classical non-symmetric Coulomb operator as well as the presented symmetric Quasi-Coulomb model. As can be seen

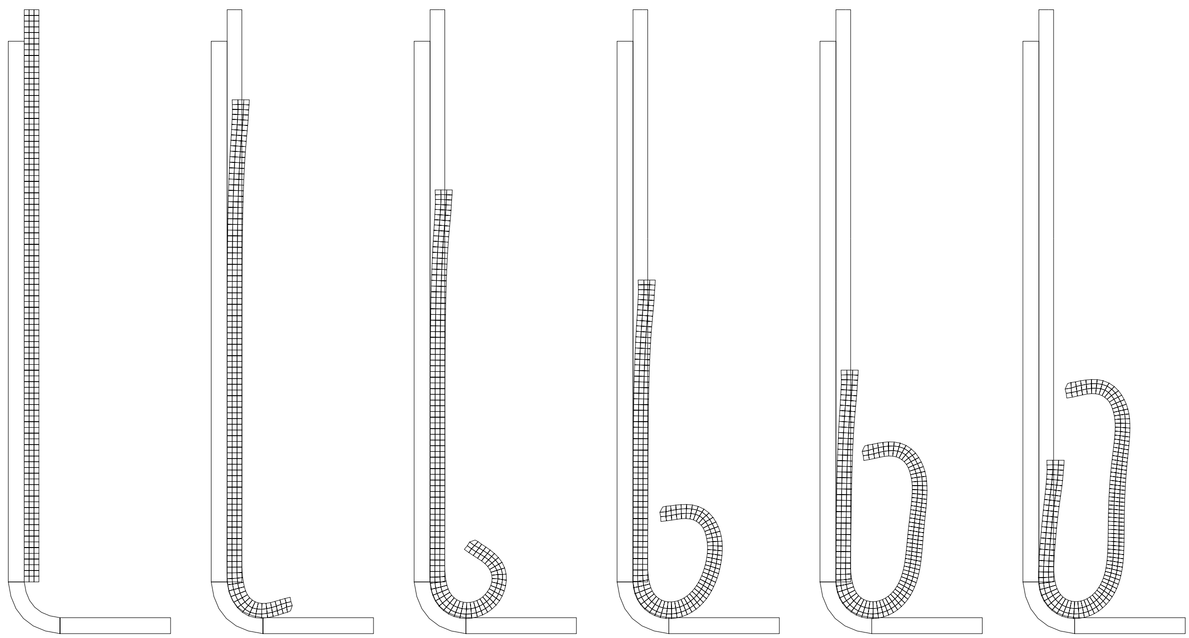

Figure 11: Deformed configurations $\mu = 0.30$ for t=0.00, t=0.25, t=0.50, t=0.75, t=1.00 and t=1.25 milliseconds.

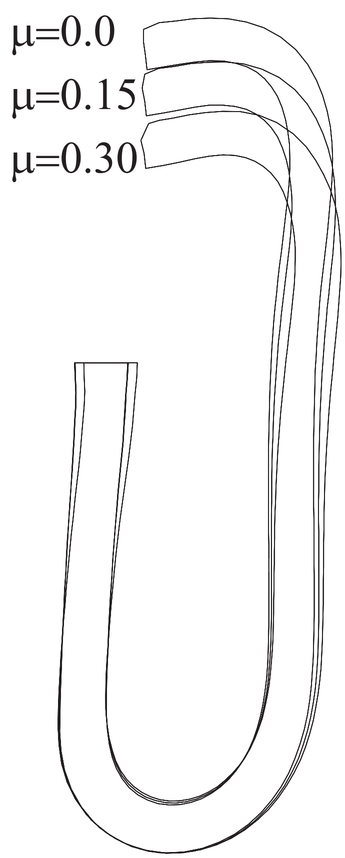

Figure 12: Comparison of the final configurations as a function of the friction coefficient.

on this figure, the proposed algorithm does not affect the results in any significant way though it retains the advantage of a symmetric solver.

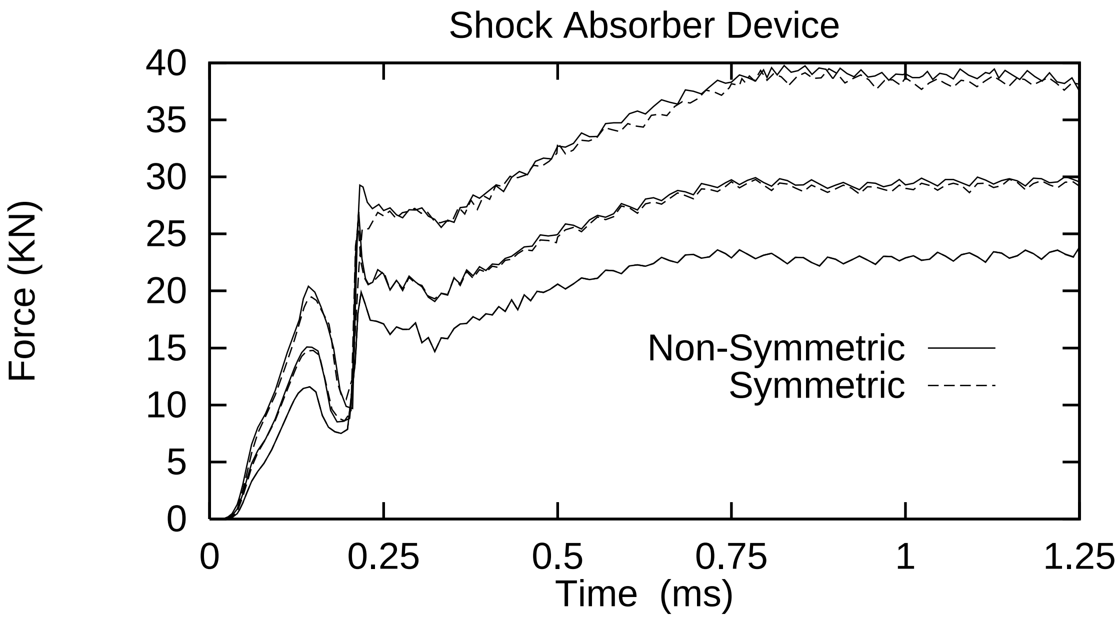

Figure 13: Applied load as a function of time. Upper curves: $\mu = 0.30$; middle curves: $\mu = 0.15$, and lower curves: $\mu = 0.00$

CONCLUSIONS

A very simple constitutive frictional model which is able to deal with both general large strain plasticity problems, as well as specialized ones such as sheet metal forming problems and crashworthiness has been presented and tested. This model is very easy to code in any non linear general purpose finite element, or finite difference, code.

In many situations, the proposed quasi-Coulomb algorithm presented here allows to use a much cheaper, symmetric solver rather than an expensive non-symmetric solver. Thus, large amounts of computational time can be saved, which is very important for industrial applications. The algorithm has been applied successfully to a sheet forming operation and to a dynamic shock absorber device simulation.

REFERENCES

[1] C. Agelet de Saracibar. *Analisis por el Método de los Elementos Finitos de Procesos de Conformado de Láminas Metálicas.* PhD thesis, E.T.S Ingenieros de Caminos, UPC, 1990.

[2] J. Huetink & F.P.T. Baaijens, editor. *Simulation of material processing: theory, methods and applications - Numiform 98*, A.A. Balkema/Rotterdam/Brookfield, 1998.

[3] K.J. Bathe, editor. *Finite Element Procedures in Engineering Analysis.* Prentice Hall, 1982.

[4] K.J. Bathe and A. Chaudary. A solution method for planar and axisymmetric contact problems. *Int. J. Num. Meth. Engng.*, 21:65–68, 1985.

[5] K.J. Bathe and A. Chaudary. A solution method for static and dynamic analysis of three-dimensional contact problems with friction. *Computers and Structures*, 24:855–873, 1986.

[6] Beltrán and Goicolea. Large strain plastic collapse: A comparison of explicit and explicit solution. In Owen R. et al., editor, *Complas II*, pages 1125–1136, Barcelona, Spain, 1989.

[7] T. Belytschko. *Computational Methods for Transient Analysis – Chapter 1 : An overview of semidiscretization and Time integration procedures.* Belytschko, T. and Hughes, T.J.R., 1983.

[8] J.-H. Chen and N. Kikuchi. An incremental constitutive relation of unilateral contact friction for large deformation analysis. *Journal of Applied Mechanics*, 52:639–648, 1985.

[9] J.L. Chenot, R.D. Wood, and O. Zienkiewicz, editors. *Simulation of material processing: theory, methods and applications - Numiform 92*, Sophia-Antipolis, France, 1992.

[10] A. Curnier. Theory of friction. *Int. J. Solids Structures*, 20(7):637–647, 1984.

[11] C. Garcí a Garino. *Un modelo numerico para el Análisis de Sólidos elastoplásticos sometidos a grandes deformaciones.* PhD thesis, E.T.S. Ingenieros de Caminos, UPC, Barcelona, 1993.

[12] C. Garcí a Garino and J. Oliver. Simulation of sheet metal forming processes using a frictional finite strain elastoplastic model. In Hirsch, editor, *First European Conference on Numerical Methods in Engineering*, pages 185–192, 1992.

[13] J.O. Hallquist. Theoretical manual for dyna3d. Technical Report UCID-19041, Lawrence Livermore National Laboratory, 1982.

[14] J.O. Hallquist. Nike2d - a vectorized implicit, finite deformation finite element code for analyzing the static and dynamic response of 2-d solids with interactive rezoning and graphics. Technical Report UCID-19677, Rev 1, Lawrence Livermore National Laboratory, 1986.

[15] T.J.R. Hughes, R.L. Taylor, J.L. Sackman, A. Curnier, and W. Kanoknukulchai. A finite element method for a class of contact-impact problems. *Comp. Meth. Appl. Mech. Engng*, 8:249–276, 1976.

[16] T.A. Laursen and J.C. Simo. Algorithmic symmetrization of coulomb frictional problems using augmented lagrangians. *CMAME*, 108:133–146, 1993.

[17] J.K. Lee, R. Wagoner, and E. Nakamachi. A benchmark test for sheet metal forming analysis. Technical report, Ohio State University, 1990.

[18] D.R.J. Owen and E Oñate, editors. *First International Conference on Computational Plasticity*, Barcelona, Spain, 1987.

[19] D.R.J. Owen and E Oñate, editors. *Second International Conference on Computational Plasticity*, Barcelona, Spain, 1989.

[20] D.R.J. Owen and E Oñate, editors. *Third International Conference on Computational Plasticity*, Barcelona, Spain, 1992.

[21] D.R.J. Owen and E Oñate, editors. *Fourth International Conference on Computational Plasticity*, Barcelona, Spain, 1994.

[22] D.R.J. Owen and E Oñate, editors. *Fifth International Conference on Computational Plasticity*, Barcelona, Spain, 1997.

[23] J.-P. Ponthot. *A Finite Element Unified Treatment of Continuum Mechanics for Solids Submitted to Large Strains.* PhD thesis, Université de Liège, Liège, Belgium, 1995. In French.

[24] J.-P. Ponthot and D. Graillet. Efficient implicit schemes for finite element impact simulation. *Submitted for publication in International Journal of Crashworthiness*, 1999.

[25] J.-P. Ponthot and M. Hogge. On relative merits of implicit/explicit algorithms for transient problems in metal forming simulations. In Kroplin et al., editor, *Numerical Methods for Metal Forming in Industry vol II*, pages 128–148, Baden Baden, 1994.

[26] S-H Shen and P. Dawson, editors. *Simulation of material processing: theory, methods and applications - Numiform 95*, A.A. Balkema/Rotterdam/Brookfield, 1995.

[27] J. C. Simo and T. Laursen. An augmented lagrangian treatment of contact problems involving friction. *Computers and Structures*, 42(1):97–116, 1992.

[28] J.C. Simo, P. Wriggers, and R.L. Taylor. A perturbed lagrangian formulation for the finite element solutions of contact problems. *Comp. Meth. Appl. Mech. Engng*, 50:163–180, 1985.

[29] P. Wriggers. On consistent tangent matrices for frictional problems. In Middleton J. Elsevier C 15/1, editor, *Numeta 87*, 1987.

[30] P Wriggers, J.C. Simo, and R.L. Taylor. Penalty and augmented lagrangian formulations for contact problems. In Middleton J., editor, *Numeta 85*, Balkema, 1985.

[31] P. Wriggers, T. Vu Van, and E. Stein. Finite element formulation of large deformation impact-contact problems with friction. *Computer and Structures*, 37(3):319–331, 1990.

[32] Z. H. Zhong and J. Mackerle. Static contact problem - a review. *Eng. Computation*, 9:3–27, 1992.

[33] O. C. Zienkiewicz and R. L. Taylor. *The finite element method, Vol 2, 4th ed.* McGraw-Hill, UK, 1989.